

# Biogenic UO<sub>2</sub> – Characterization and Surface Reactivity

David M. Singer<sup>1</sup>, François Farges<sup>1,2</sup>, Gordon E. Brown, Jr.<sup>1,3</sup>

1. *Surface and Aqueous Geochemistry Group, Department of Geological and Environmental Sciences, Stanford University, 450 Serra Mall, Building 320, Stanford, California, 94305-2115, USA*
2. *Laboratoire de Minéralogie, Muséum National d'Histoire Naturelle, CNRS UMR 7160, Paris, France*
3. *Stanford Synchrotron Radiation Laboratory, SLAC, MS 69, 2575 Sand Hill Road, Menlo Park, California, 94025, USA*

**Abstract.** Nano-scale biogenic UO<sub>2</sub> is easier to oxidize and more reactive to aqueous metal ions than bulk UO<sub>2</sub>. In an attempt to understand these differences in properties, we have used a suite of bulk and surface characterization techniques to examine differences in the reactivity of biogenic UO<sub>2</sub> versus bulk UO<sub>2</sub> with respect to aqueous Zn(II). Precipitation of biogenic UO<sub>2</sub> was mediated by *Shewanella putrefaciens* CN32, and the precipitates were washed using two protocols: (1) 5% NaOH, followed by 4 mM KHCO<sub>3</sub>/KCl (NA-wash; “NAUO<sub>2</sub>”, to remove surface organic matter), and (2) 4 mM KHCO<sub>3</sub>-KCl (BI-wash; “BIUO<sub>2</sub>”, to remove soluble uranyl species). BET surface areas of biogenic-UO<sub>2</sub> prepared using the two protocols are 128.63 m<sup>2</sup>g<sup>-1</sup> and 92.56 m<sup>2</sup>g<sup>-1</sup>, respectively; particle sizes range from 2-10 nm as determined by FEG-SEM. Surface composition was probed using XPS, which showed a strong carbon 1s signal for the BI-washed samples; surface uranium is > 90% U(IV) for both washing protocols. U L<sub>III</sub>-edge XANES spectra also indicate that U(IV) is the dominant oxidation state in the biogenic UO<sub>2</sub> samples. Fits of the EXAFS spectra of these samples yielded half the number of uranium second-shell neighbors relative to bulk UO<sub>2</sub>, and no detectable oxygen neighbors beyond the first shell. At pH 7, the sorption of Zn(II) onto both biogenic and bulk UO<sub>2</sub> is independent of electrolyte concentration, suggesting that Zn(II) sorption complexes are dominantly inner-sphere. Fits of Zn K-edge EXAFS spectra for biogenic UO<sub>2</sub> indicate that Zn(II) sorption is dependent on the washing protocol. Zn-U pair correlations are observed for the NA-washed samples, but not for the BI-washed ones, suggesting that Zn(II) sorbs directly to the UO<sub>2</sub> surface in the first case, and possibly to organic matter in the latter. Further work is required to elucidate the binding mechanism of Zn(II) to bulk UO<sub>2</sub>.

**Keywords:** Biogenic UO<sub>2</sub>, nanoparticles, metal-reducing bacteria, XAFS

**PACS:** 78.70.Dm

## INTRODUCTION

UO<sub>2</sub> is found in natural ore deposits, spent nuclear fuel waste repositories, and in redox permeable reactive barriers designed to promote uranium reduction through abiotic and biologically mediated processes [1]. With regard to biological processes, metal-reducing bacteria can reduce soluble and mobile U(VI) to U(IV), which precipitates as UO<sub>2</sub> [2]. The surface reactivity of biologically precipitated UO<sub>2</sub> must be evaluated in order to determine the short- and long-term stability of biogenic UO<sub>2</sub>, and the conditions that could result in the re-release of soluble uranium. While the processes that control enzymatic reduction of uranium have been well studied, the stability and reactivity of the biogenic UO<sub>2</sub> product has not been considered, particularly with respect to the nano-scale size of biogenic UO<sub>2</sub> [3]. A number of studies have dealt with the fate of bulk UO<sub>2</sub> in the environment [4].

Although biogenic UO<sub>2</sub> shares some basic properties with bulk UO<sub>2</sub>, there are also likely significant differences, including different solubilities and different surface reactivity with respect to aqueous metal ions [3]. Several surface and bulk characterization techniques were used to determine the physical and chemical nature of biogenic UO<sub>2</sub>. In order to probe the internal structure of biogenic UO<sub>2</sub>, we employed powder X-ray diffraction (XRD) and synchrotron based U L<sub>III</sub>-edge X-ray Absorption Fine Structure (EXAFS) spectroscopy. Batch sorption of Zn(II) to biogenic and abiotic UO<sub>2</sub> was used to determine the potential differences in surface reactivity of the two phases, and the resulting Zn(II) sorption complexes were characterized with Zn K-edge EXAFS.

## METHODS AND MATERIALS

Precipitation of biogenic  $\text{UO}_2$  was mediated by *Shewanella putrefaciens* CN32, adapted from Wielinga et al. (2000) [5]. Biogenic  $\text{UO}_2$  was washed using one of two protocols; half the material (NAUO<sub>2</sub>) was washed with 5 % NaOH followed by 4 mM KHCO<sub>3</sub>-KCl (at pH 7) to remove all organic material and residual aqueous uranyl. The other half (BIUO<sub>2</sub>) was washed with 4 mM KHCO<sub>3</sub>-KCl (at pH 7), to remove residual aqueous uranyl. Both sets of material were finally washed with anaerobic distilled/deionized water before surface and bulk characterization. BET surface area was determined using an N<sub>2</sub> isotherm and dry samples were analyzed by X-ray diffraction (XRD) and X-ray photoelectron spectroscopy (XPS).

$\text{U L}_{\text{III}}$ -edge and Zn K-edge XAFS spectra were collected at the Stanford Synchrotron Radiation Laboratory (SSRL), on beamline 11-2 at 298 K, using a cryogenically cooled double-crystal Si (220) monochromator ( $\phi = 90^\circ$  for the  $\text{U L}_{\text{III}}$ -edge or  $\phi = 0^\circ$  for the Zn K-edge). Fluorescence-yield EXAFS data at the  $\text{U L}_{\text{III}}$ -edge were collected using a Lytle detector, filled with Kr gas. Fluorescence-yield EXAFS data at the Zn K-edge were collected using a 13-element solid-state germanium detector. The edge positions of the XANES spectra were set as the half-height of the normalized adsorption maximum. EXAFS spectra were extracted from the averaged data files by preedge subtraction followed by spline fitting using SixPack [6]. Background-subtracted  $k^3$ -weighted EXAFS were analyzed using the SixPack interface to IFEFFIT [7]. Phase-shift and amplitude functions for quantitative EXAFS fitting were generated using FEFF 7 [8], from the crystal structures of uraninite [9] and zinc nitrate hexahydrate [10]. The amplitude reduction function,  $S_0^{-2}$  was set at 0.90 and 0.92 for the  $\text{U L}_{\text{III}}$ -edge, and Zn K-edge, respectively.

## RESULTS AND DISCUSSION

The BET surface area determined using a N<sub>2</sub> isotherm for NAUO<sub>2</sub>, BIUO<sub>2</sub>, and bulk UO<sub>2</sub> are 128.63, 92.56, and 3.90 m<sup>2</sup>g<sup>-1</sup>, respectively. FEG-SEM confirmed that particle size of biogenic UO<sub>2</sub> is on the order of 2-10 nm. XPS analysis indicated that the surface of biogenic UO<sub>2</sub> is > 90% U(IV), and that the NA-wash protocol removed organic material associated with the particle surface, while the BI-wash protocol did not. The XRD pattern of biogenic UO<sub>2</sub> showed broadened diffraction peaks relative to bulk UO<sub>2</sub>, indicative of small particles and/or structural disorder in the former.

$\text{U L}_{\text{III}}$ -edge XANES also indicated that biogenic UO<sub>2</sub> is nearly 100% U(IV). The edge position is

independent of washing treatment, or age (2 months old samples).  $\text{U L}_{\text{III}}$ -edge EXAFS also showed no differences for biogenic UO<sub>2</sub> samples that were subject to the two washing treatments, or that were aged. EXAFS fits (Figure 1) indicate that the number of U-U pair correlations decreases from  $12 \pm 1$  in bulk UO<sub>2</sub> to  $7 \pm 1$  in biogenic UO<sub>2</sub>. No detectable second-shell oxygen neighbors were found in the biogenic UO<sub>2</sub> (Table 1). There is also an increase in static disorder, a change in interatomic distances for all shells, and a more significant contribution of multiple scattering for biogenic UO<sub>2</sub>, which arise from U-O-U-O scattering at 4.7 Å. These results compare well to previously published results of nanoparticulate UO<sub>2</sub> [11]; however, we have found a smaller contribution from multiple-scattering compared to this earlier EXAFS study.

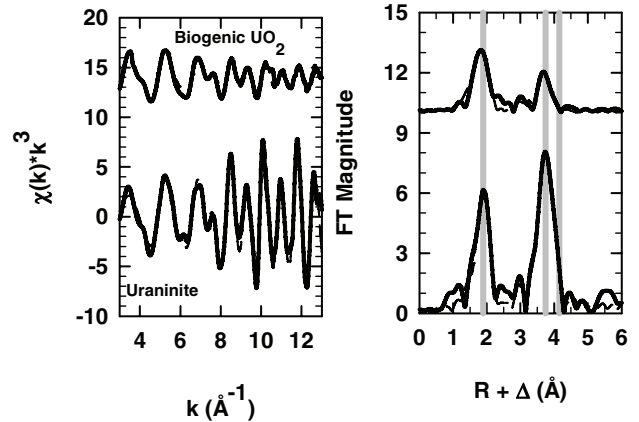


**FIGURE 1.**  $\text{U L}_{\text{III}}$ -edge EXAFS (left) and Fourier Transform (right) of uraninite and biogenic UO<sub>2</sub>. Experimental data and their best fits are in solid dashed lines, respectively. The vertical grey lines represent, from left to right, the position of the first oxygen, uranium, and second oxygen shells.

**TABLE 2.**  $\text{U L}_{\text{III}}$ -edge EXAFS fit results.

path	N <sub>XRD</sub> *	N <sub>EXAFS</sub>	R <sub>XRD</sub> * (Å)	R <sub>EXAFS</sub> (Å)	σ <sup>2</sup> (Å <sup>2</sup> )
biogenic UO2					
U-O	-	8(1)	-	2.35(1)	0.012(1)
U-U	-	7(1)	-	3.85(1)	0.009(1)
MS*	-	16(6)	-	4.7(1)	0.01(1)
uraninite					
U-O1	8	8(1)	2.36	2.36(1)	0.006(1)
U-U	12	12(1)	3.87	3.87(1)	0.005(1)
U-O2	24	25(6)	4.53	4.49(3)	0.009(4)

\*Wyckoff (1963) \*\*MS = multiple scattering: U-O1-U-O1

Zn(II) sorption on biogenic UO<sub>2</sub>, at pH 7, was independent of the electrolyte concentration, suggesting that Zn(II) sorption is controlled by an inner-sphere mechanism. Zn(II) sorption is also independent of the washing treatment used. Fits of the Zn K-edge EXAFS (Figure 2) of the sorption samples support the results of the batch uptake experiment. Sorption sample A (NAUO<sub>2</sub> substrate with 1 mM Zn(II), and 100 mM NaCl) was modeled with a slightly disordered first shell of six oxygen atoms at 2.10 Å. A third cumulant term was required to account for slight anharmonicity (Table 2). The fit also includes one U atom at 2.78 Å, supporting the conclusion of dominantly inner-sphere complexes on the biogenic UO<sub>2</sub> surface from the batch Zn(II) uptake studies. Sample B (BIUO<sub>2</sub> substrate, 1 mM Zn, and 100 mM NaCl) was also fit with a slightly disordered first shell of six oxygen atoms at 2.10 Å. However, no nearest neighbors beyond the first shell were detected for this sample. Given that the batch uptake results suggest a dominantly inner-sphere sorption mechanism, the sorption of Zn(II) to organic matter on the biogenic UO<sub>2</sub> surface would result in carbon nearest neighbors, that would be difficult to detect by EXAFS methods. Due to the low surface area of bulk UO<sub>2</sub>, Zn(II) loading was not high enough to obtain a Zn K-edge EXAFS spectrum, and further work will include higher Zn(II) loadings.

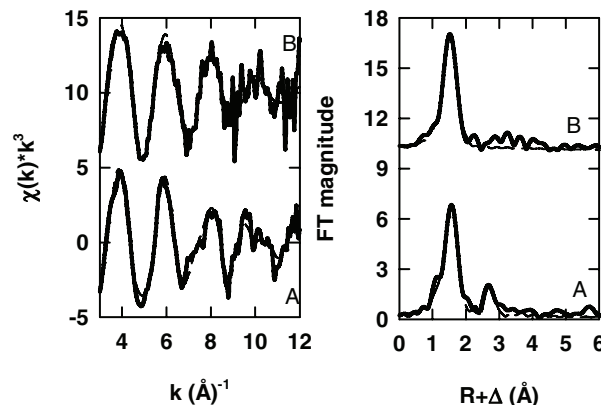


**FIGURE 2.** Zn K-edge EXAFS (left) and Fourier Transform (right) of sorption samples A and B. Experimental data and their best fits are in solid dashed lines, respectively.

**TABLE 2.** Zn-edge EXAFS fit results.

path	N	R ( $\text{\AA}$ )	$\sigma^2 (\text{\AA}^2)$	$\sigma^3 (\text{\AA}^3)$	$\Delta E^0$	red. $\chi^2$
Sample A						
Zn-O	6.0(6)	2.11(2)	0.011(1)	0.0011(4)	5(1)	28.5
Zn-U	0.8(1)	2.76(2)	0.007(2)	-		
Sample B						
Zn-O	5.9(3)	2.10(2)	0.011(1)	0.0015(4)	6(1)	5.0

The preliminary results presented here suggest that remnant biological material on the surfaces of biogenic UO<sub>2</sub> can significantly change its surface reactivity. Also, the absence or presence of organic matter needs to be taken into account when studying the sorption and sequestration of metal ions on biogenic UO<sub>2</sub>. Further work is required to elucidate the binding mechanism of Zn(II) to bulk UO<sub>2</sub>, in order to determine the types of reactive sites on uraninite compared to biogenic UO<sub>2</sub>.

## ACKNOWLEDGMENTS

This research has been funded by the National Science Foundation through grant CHE-0431425 (the Stanford Environmental Molecular Science Institute). We thank John Bargar (SSRL) and Joe Rogers (SSRL) for their beamline support during data collection, and the staff of SSRL for their continual support. We also thank Matthew Ginder-Vogel (Stanford) for assistance with preparation of biogenic UO<sub>2</sub>, Bob Jones (Stanford) for assistance with FEG-SEM, and Mike Kelly (Stanford) for assistance with XPS. SSRL is funded by the U.S. Department of Energy and the National Institutes of Health.

## REFERENCES

1. E.M. Pierce, J.P. Icenhower, R.J. Serne *et al.*, *J. Nucl. Mat.* **345**, 206 (2005).
2. D. R. Lovley, E. J. P. Phillips, Y. A. Gorby *et al.*, *Nature* **350** (6317), 413 (1991); Y. A. Gorby and D. R. Lovley, *Env. Sci. Tech.* **26**, 205 (1992).
3. Y. Suzuki, S.D. Kelly, K.M. Kemner *et al.*, *Nature* **419**, 134 (2002).
4. G.A. Parks and D. Pohl, *Geochim. Cosmochim. Acta* **52**, 863 (1988); J. Bruno, I. Casas, and I. Puigdomenech, *Geochim. Cosmochim. Acta* **55**, 647 (1991); I. Casas, J. de Pablo, J. Gimenez *et al.*, *Geochim. Cosmochim. Acta* **62** (13), 2223 (1998).
5. B. Wielinga, B. Bostick, C. Hansel *et al.*, *Env. Sci. Tech.* **34**, 2190 (2000).
6. S. Webb, *Physica Scripta* **T115**, 1011 (2004).
7. M. Newville, *J. Synchrotron Rad.* **8**, 322 (2001).
8. J.J. Rehr, R.C. Albers, and S.I. Zabinsky, *Phys. Rev. Lett.* **69** (23), 3397 (1992).
9. R.W.G. Wyckoff, *Crystal Structures 1 Second edition*. (Interscience Publishers, New York, New York, 1963).
10. A. Ferrari, A. Braibanti, A.M.M. Lanfredi, and A. Tiripicchio, *Acta Crystallogr. A* **22**, 240 (1967).
11. E.J. O'Loughlin, S.D. Kelly, R.E. Cook *et al.*, *Env. Sci. Tech.* **37**, 721 (2003).